Letter

Fitness landscape for quantum state tomography from neutron scattering

Tymoteusz Tula, Jorge Quintanilla,* and Gunnar Möller†
Physics of Quantum and Materials Group, School of Engineering, Mathematics and Physics, University of Kent, Canterbury, Kent CT2 7NH, United Kingdom

(Received 27 January 2025; accepted 15 July 2025; published 16 October 2025)

Recently, a direct connection between static structure factors and quantum ground states for two-spin interaction Hamiltonians was proven. This suggests the possibility of quantum state tomography from neutron scattering. Here, we investigate the associated fitness landscape numerically. We find a linear relationship between the mean-square distances of structure factors and associated state overlaps, implying a well-behaved fitness landscape. Furthermore, we find evidence suggesting that the approach can be generalized to thermal equilibrium states. We also extend the arguments to the cases of applied magnetic fields and finite clusters.

DOI: 10.1103/x9mb-x1gz

The large number of degrees of freedom in condensed matter systems can make obtaining detailed microscopic insights from experimental data challenging. Usually a model Hamiltonian $\hat{H}$ is used to predict the state of the system in the form of a ground-state wave function ψ_0 (or, more generally, a thermal density matrix ρ). Once the state is known, the expectation value of an observable $\hat{O}$ can be evaluated using a known ground-state functional, $\langle\hat{O}\rangle = \langle\psi_0|\hat{O}|\psi_0\rangle$ (more generally, $\langle\hat{O}\rangle = \mathrm{Tr}\,\rho\hat{O}$). A comparison to the experiment is then used to refine the model $\hat{H}$. In general, however, the relationships $\hat{H} \to \langle\hat{O}\rangle$ and $\psi_0 \to \langle\hat{O}\rangle$ ($\rho \to \langle\hat{O}\rangle$) are not invertible: There is no guarantee of a unique model $\hat{H}$, or even a unique ground state (or density matrix) compatible with a given observation. A prominent counterexample is provided by Hohenberg and Kohn's theorem, stating that knowledge of the density distribution uniquely determines the ground state of the system [1], providing the latter is nondegenerate. Generalizing this point of view, the prefactors of any unknown terms in the Hamiltonian are fully constrained if the corresponding ground-state or thermal correlation functions are known [2]. Recently, one of us has highlighted that this enables the learning of Hamiltonian parameters of systems with exclusively pairwise interactions of spins where the observable is the ground-state magnetic structure factor $S_{\alpha,\beta}(\mathbf{q})$ [3], as well as proving that the many-body wave function can also be inferred directly from the ground-state correlators. The proof of the former, and a weaker form of the latter, have been generalized to finite temperatures [4].

Crucially, the magnetic structure factor is experimentally accessible via diffuse magnetic neutron scattering. This offers the prospect, *in principle*, of using diffuse magnetic scattering on a quantum magnet to completely determine its wave function (quantum state tomography) or its Hamiltonian (Hamiltonian learning). Compared to other schemes aiming to determine states [5,6] or Hamiltonians [7–12] from local measurements that have been discussed in the context of quantum simulators, this has the advantage that it does not require the full covariance matrix [7–10] and that all the necessary correlators are determined simultaneously in the neutron-scattering measurement, so there is no scaling of experimental complexity [12] with the size of the system or the range of interactions.

The main purpose of the present Letter is to determine whether the above scheme could work *in practice*. To address this question, we study how the normalized difference between random trial scattering functions and a given target scattering function varies as the trial state moves away from the target. The ensemble of rms differences across a large set of trial states represents a "fitness landscape" for the inverse neutron-scattering problem (according to Theorem 2 in Ref. [3]). We numerically explore both the zero- and finite-temperature cases. We also generalize previous discussions [3,4] to the case where there are applied magnetic fields and provide further evidence of the validity of the theorems at finite temperature.

General framework. We first provide key definitions to set up the general framework and choice of models we consider. Specifically, we define appropriate metrics in the spaces of scattering functions and quantum states. We will assume the Hamiltonian is of the class considered in Refs. [3,4], featuring only two-spin interactions,

$$H_J = \sum_{i,j}\sum_{\alpha,\beta} J_{i,j}^{\alpha,\beta} S_i^\alpha S_j^\beta, \tag{1}$$

where operators S_i^α represent spin components along axis $\alpha \in x, y, z$ at site i of the lattice, and $J_{i,j}^{\alpha,\beta}$ are a completely generic set of coupling constants between these. Note that this form does not include linear terms. Meanwhile, in the experimental setup, one cannot exclude local magnetic fields affecting the state of the system. Indeed, such fields are often an important tool to explore the physics of a given material. For instance, they can be used to tune a material to quantum criticality

*Contact author: J.Quintanilla@kent.ac.uk
†Contact author: G.Moller@kent.ac.uk

[13,14]. Our first result is a proof that the class of generic spin Hamiltonians described by Eq. (1) in fact includes all Hamiltonians with local fields,

$$H_{J+h} = \sum_{i,j}\sum_{\alpha,\beta} J_{i,j}^{\alpha,\beta} S_i^\alpha S_j^\beta + \sum_i \sum_\alpha h_i^\alpha S_i^\alpha, \tag{2}$$

if we allow the coupling constants $J_{i,j}^{\alpha,\beta}$ in Eq. (1) to be complex. A proof follows straightforwardly by noting that the commutators of products of two spin operators on the same site naturally generate imaginary single-spin terms. We give a detailed proof in the Supplemental Material [15]. In our numerical study we will therefore include systems of the form (2) with real exchange constants $J_{i,j}^{\alpha,\beta}$ and magnetic fields h_i^α.

Our methodology of testing the fitness landscape of scattering functions can be summarized as follows: First, we select a reference Hamiltonian H describing a chain of L sites $S = \frac{1}{2}$. Calculating either a ground state ψ, or thermal density function $\rho(\beta)$ allows us to evaluate the full diffuse magnetic scattering function $\mathcal{S}(\mathbf{q})$ for the reference Hamiltonian. Then we proceed to add random variations to the ground state/density function, $\psi' = \psi + \delta\psi$, $\rho' = \rho + \delta\rho$, and evaluate the scattering functions $\mathcal{S}'(\mathbf{q})$ that are obtained from the new states. By defining a metric for the distance between two scattering functions $\Delta\mathcal{S}(\mathcal{S}, \mathcal{S}')$ (chosen as a properly normalized mean-square deviation), we can study the relationship of $\Delta\mathcal{S}$ with the distance between the respective states by examining multiple samples of random variations $\delta\psi$ or $\delta\rho$. Overlaps induce a natural metric in state space; for further details see the Supplemental Material [15].

State tomography. We now present the results of our investigation into the fitness landscape for quantum state tomography in magnets. A first overview is given in Fig. 1. In Fig. 1(a), we illustrate the relation between the distance $\Delta\mathcal{S}$ of random states from the target scattering function against their state distance [15] for a molecular magnetic tetramer ($L = 4$) comprising four spin-$\frac{1}{2}$ described by the antiferromagnetic Heisenberg with nearest-neighbor interactions of fixed strength J in a ring geometry. Random state vectors were created by adding Gaussian noise terms of width σ to each component of the target state vector, followed by normalization [15]. We display groups of results for three distinct maximal widths $\sigma_{\max}$. Similar results were obtained using uniform noise distributions (not shown). Figure 1(a) shows a clear correlation between $\Delta\mathcal{S}$ and $\mathrm{dist}(\psi, \psi')$.

To gain some intuition, we also provide examples of scattering functions, including Fig. 1(b) for the target ground state and Figs. 1(c)–1(e) for three of the randomly drawn states, hand-picked for representativeness [marked by stars in Fig. 1(a)]. The differences in the scattering functions are clearly appreciable by eye, even for the state in Fig. 1(c) that is closer to the target. The scattering function in Fig. 1(c) is about 15% from the target while the wave-function overlap deviates by ∼5%. This suggests that it is possible to determine the system's ground state with considerable precision using realistically noisy neutron-scattering data. We also note that the candidate function in Fig. 1(c) has, to a very good approximation, the same fourfold symmetry as the target function, in contrast to the candidates with smaller overlaps, which look qualitatively different. This is a trend we see in all our simulations. These observations have practical implications: On the one hand, when symmetry constraints or other qualitative features of the data are known, including them can accelerate the search for the target state and improve its accuracy. On the other hand, our results show that an unbiased search through the Hilbert space may yield states with the correct features even if these are not known *a priori* and the experimental and target scattering functions can only be determined with limited accuracy.

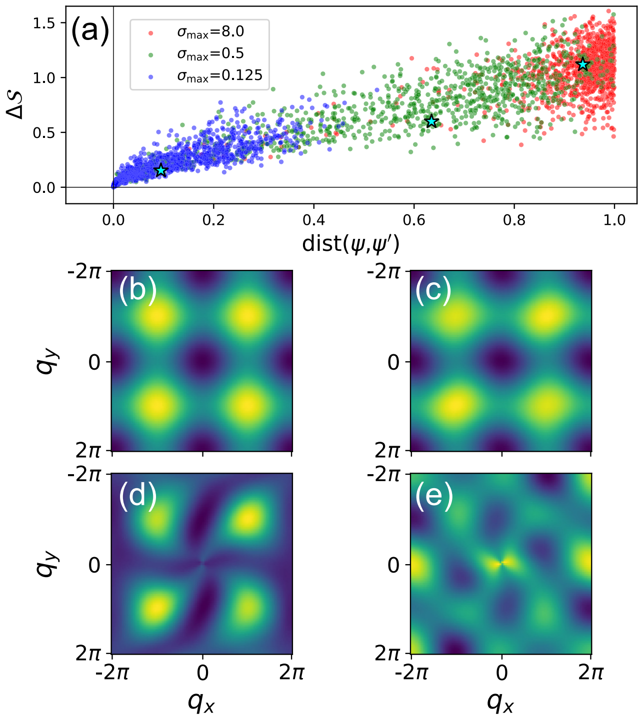

FIG. 1. Fitness landscape for quantum state tomography using the ground state's diffuse magnetic neutron-scattering function. The target state ψ is the ground state of a spin-$\frac{1}{2}$ ring tetramer ($L = 4$) with nearest-neighbor, antiferromagnetic Heisenberg interactions. (a) Cost function $\Delta\mathcal{S}$ as a function of the distance $\mathrm{dist}(\psi, \psi')$ of the trial state vectors ψ' to the target ground state [15]. We display three sets of 1000 random state vectors each, with amplitudes drawn from Gaussian distributions centered on ψ. The color legend indicates the maximum standard deviation $\sigma_{\max}$ used for the set, while each trial state is marked by a solid circle and has components generated from distribution with a random width σ, where $0 < \sigma < \sigma_{\max}$ [15]. (b) The target diffuse magnetic scattering function $\mathcal{S}(\mathbf{q})$ for the exact ground state. (c)–(e) Three scattering functions obtained from the three random states highlighted with stars on (a), in order of increasing state distance.

Next, we study antiferromagnetic Heisenberg rings of different lengths $L = 4, 6, 8, 10, 12, 14$, employing a size-dependent width in the noise distributions for good data coverage [15]. Figure 2(a) shows that as L increases, the scatter in the data reduces, and they cluster around a single sharply defined curve. Remarkably, a simple linear relationship with a coefficient equal to unity describes this curve very well:

$$\Delta\mathcal{S} = \mathrm{dist}(\psi, \psi'). \tag{3}$$

Our results further suggest that trial states ψ' approaching the target ψ are more likely to obey the remarkably simple

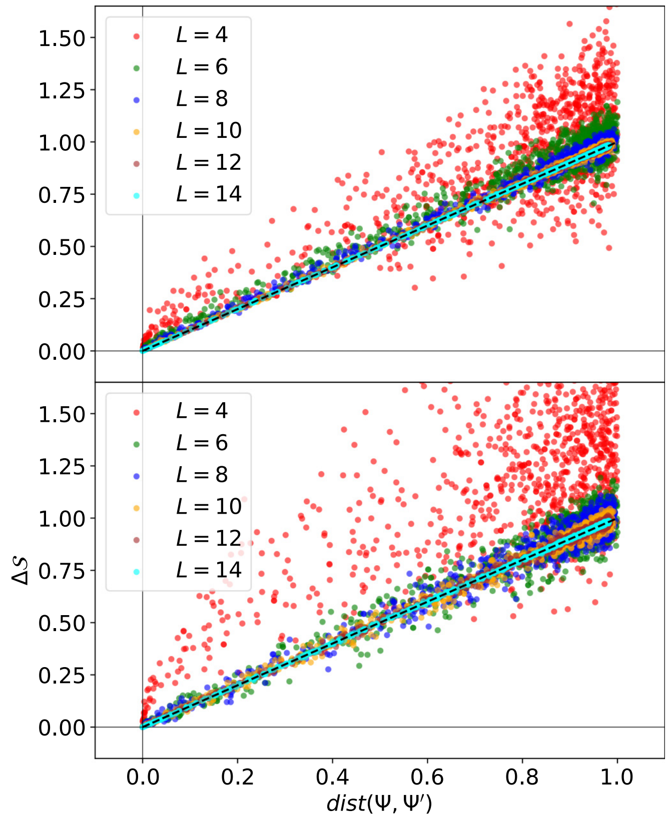

FIG. 2. Dependence of the fitness landscapes on the number of spins L in the cluster. For each L, 1000 target states were sampled with normal-distributed perturbations around the target wave function (see main text). Target states were chosen as ground states of (a) a spin-$\frac{1}{2}$, nearest-neighbor antiferromagnetic Heisenberg model in a ring geometry, i.e., the same model as in Fig. 1, but with varying L. (b) A random long-range spin-$\frac{1}{2}$ Hamiltonian in a linear open chain geometry, given by Eq. (2) with random exchange constants $J_{i,j}^{\alpha,\beta}$ and a random global magnetic field with components $h_i^\alpha = h^\alpha$. For each L, Hamiltonian parameters $J_{i,j}^{\alpha,\beta}$ and h^α were drawn from a normal distribution with zero average and standard deviation equal to J [the nearest-neighbor coupling of the Heisenberg Hamiltonian used in (a)]. Dashed lines in (a) and (b) show the linear relation in Eq. (3).

law (3). This indicates an easy-to-navigate fitness landscape: Once we are in the vicinity of the target scattering function, there is a well-defined slope towards the target state. This is a remarkable result and constitutes our main finding. The fact that the "empirical" law (3) is independent of L encourages us to conjecture the relationship will hold even in the thermodynamic limit.

In the above discussion, we used the antiferromagnetic Heisenberg model with nearest-neighbor interactions to generate our target ground state. This was selected as a well-known textbook example for quantum magnets. The ring geometry was inspired by molecular quantum magnets which are experimental realizations of finite-size magnetic clusters amenable to treatment by exact diagonalization and quantum eigensolvers [16,17]. However, our conclusions are robust to variations in the the model and geometry. To illustrate this, Fig. 2(b) shows results for a linear molecule with randomly chosen coupling constants and an externally applied field of arbitrary strength and direction. In addition to the different geometry, these models lack SU(2) and time-reversal symmetries. Moreover, the couplings are defined on a fully connected graph with no natural length scale. Thus, as L grows the model can no longer be considered one dimensional. Finally, we note that such random Hamiltonians typically have competing ferromagnetic and antiferromagnetic couplings. In spite of all these differences, we obtain very similar behavior. These results also confirm our proof shown above and in the Supplemental Material [15] that the arguments in Ref. [3] can be extended to pairwise-interacting spin models with an externally applied magnetic field. Moreover, they strongly suggest that the linear relationship (3) describing the fitness landscape for quantum tomography in the vicinity of a target ground state applies universally. Our results in Fig. 2(b) additionally demonstrate that the inverse scattering problem can be solved even for a nonperiodic magnetic structure. We extend the arguments of Ref. [3] and formally prove the possibility of quantum tomography for nonperiodic structures or finite-size clusters in the Supplemental Material [15].

Finite temperature. In the foregoing we have shown numerical evidence that the $T = 0$ ground states of pairwise coupled spin models can be inferred from neutron-scattering data. Is the same true for magnetic systems at finite temperatures? In fact, while Hamiltonian learning from structure factors was proven to be possible at $T > 0$ [4], so far no extension for state tomography to thermal density matrices was found [18]. Nevertheless, we can apply the same *numerical* analysis as for the ground state, to check whether there is any numerical evidence to suggest that the relationship from finite-T density matrices to the structure factor is also invertible. We test this hypothesis by sampling random, positive-definite density matrices in the vicinity of the thermal equilibrium density matrix of a given target Hamiltonian with normal-distributed long-range couplings (for details, see Supplemental Material [15]).

The resulting data are shown in Fig. 3, numerically supporting the hypothesis. The most salient feature, compared to the zero-T cases in Fig. 2, is the much steeper (sublinear) increase in ΔS with increasing interstate distance dist(ρ, ρ'). This is due to the fact that the space of trial density matrices ρ' is of higher dimensionality than that of trial pure states ψ'. Even if we choose the target state to be arbitrarily close to the ground state (by choosing the target temperature to be very low, compared to all the Hamiltonian parameters) we still find this markedly sublinear behavior, as the ρ' matrices almost never represent pure states such as those considered earlier. Additionally, we find that the prefactor of the sublinear scaling depends on the random choice for the target Hamiltonian (see the inset illustrating the data for a distinct set of randomized target Hamiltonians).

Discussion and conclusions. In this Letter we have presented an exact diagonalization study of the fitness landscape for static magnetic structure factors of many-spin Hamiltonians with pairwise interactions, both in the ground state and at finite temperature. Our results allow us to assess the practicality of quantum state tomography based on diffuse magnetic neutron scattering.

Our results include the important cases when there is a magnetic field applied to the sample. This was achieved

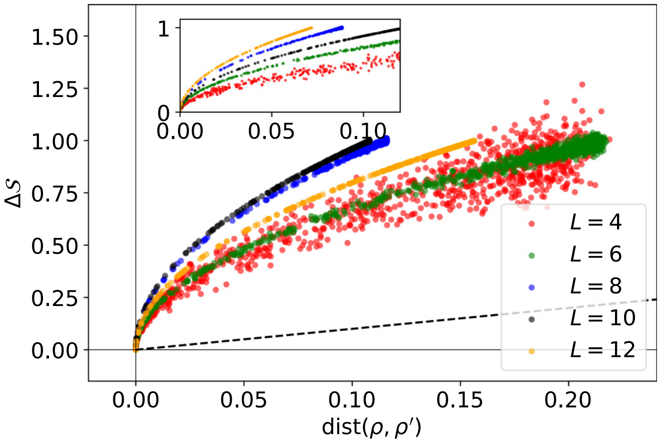

FIG. 3. Dependence on L (see legend) of the fitness landscape for finite-temperature quantum tomography for a model with random long-range interactions. The target Hamiltonian and geometry are defined in the same way as in Fig. 2(b). The target density matrix ρ is the thermal equilibrium density matrix of that Hamiltonian at temperature $T = J$. One thousand trial configurations (random density matrices) were tested against this target, based on adding noise terms followed by restoring positive definiteness and normalization [15]. The horizontal axis shows a distance between random density matrices that for $T = 0$ would have coincided with the overlap-induced distance dist(ψ, ψ') between ground states [15]. The dashed line represents Eq. (3), for comparison. The inset shows similar output with different random targets at each size.

through an analytical transformation between Hamiltonians with linear terms and purely quadratic Hamiltonians with complex interaction constants [15]. This result extends the validity of our study and the theorems that underpin it [3,4] and is our first result.

Our results for the fitness landscape indicate that the cost functions for quantum tomography from structure factors are well behaved, both in the ground state and at finite temperature, with no evidence of barren plateaus or local minima. This is our second main result, and the core result in this Letter. Third, we proved that tomography is possible even from the structure factors of nonperiodic magnetic clusters [15].

The case of quantum tomography at finite temperature deserves special attention. The proofs of the one-to-one correspondences between Hamiltonians and correlators (Theorem 1 in Ref. [3]) and between wave functions and correlators (Theorem 2) are based on the Rayleigh-Ritz variational principle [19], which is used by many numerical techniques, such as density functional theory (DFT) [20], variational Monte Carlo methods [21], or recent artificial intelligence methods [22]. The principle states that given a Hamiltonian H, the ground state will minimize the energy globally, which means that $E(\psi) = \langle\psi|H|\psi\rangle/\langle\psi|\psi\rangle$ is a good optimization function for finding ground states. Their generalizations to systems at finite temperatures require using a similar inequality applied to thermal density matrices known as the Gibbs-Delbrück-Moliére quantum variational principle [23] (or, equivalently, the Gibbs-Bogoliubov inequality). In this case, the objective function is the free energy, defined by

$$F(\rho) = \mathrm{Tr}[\rho H] - \beta^{-1}\,\mathrm{Tr}[\rho \ln \rho], \tag{4}$$

consisting of terms corresponding to expectation values of the energy and entropy, respectively. The free energy (4) is minimized for the thermal density matrix $\rho = e^{-\beta H}/\mathrm{Tr}[e^{-\beta H}]$. It turns out that the entropy term does not alter the reasoning of the proof of Theorem 1, as shown by Murta and Fernández-Rossier [4]. However, as noted in that reference, that does not carry over to Theorem 2: One cannot discard the possibility that there are density matrices with lower entropy than the real ones which reproduce the experimental data. However, the systematic numerical exploration presented in the present Letter did not provide any examples of this, giving strong indication that such cases, if they exist, must be special, at least for finite-size systems. This is the fourth principal result of the present study.

Finally, we note the advantage of using experimental neutron-scattering data as an input, rather than real-space correlators. At a mathematical level, both inputs are closely related due to their linear relation and arguments related to Parseval's theorem of Fourier analysis (see Appendix A in Ref. [3] for the proof in the case of translational-invariant systems and the Supplemental Material [15] for the extension to finite clusters), so our approach would operate similarly on both input data. However, experimental approaches giving access to the spatial two-site correlation functions, including experiments with cold atoms/ions [24–26] or potentially surface measurements using local probes [27–30], typically require separate measurements for each pairwise correlator and, for the latter, probe only surface states. In contrast, as discussed in Ref. [3], neutron scattering yields information about the bulk wave function of the material in a single shot.

Our results suggest that the variational approach to quantum magnets proposed in Ref. [3], where an efficient representation of the wave function of a magnet is optimized to reproduce experimentally obtained neutron-scattering data, may be feasible, at least for magnets formed of finite-size clusters. Additional studies will be necessary to ascertain whether this conclusion carries over to fully connected systems as well as the effect of noisy and incomplete data sets. Effective ways to represent the wave function, for instance, using neural networks, tensor networks, or quantum circuits (and the potential of the latter to achieve scaling advantages when implemented on noisy, intermediate-scale quantum hardware) will also need to be developed.

Acknowledgments. G.M. acknowledges insightful discussions with F. Verstraete, who pointed out that our results are supported by a geometric interpretation, namely that the ensemble of possible expectation values in thermal equilibrium form a convex set in observable space [31]. T.T. is supported by the EPSRC via a DTA studentship under Grant No. EP/R513246/1 and by the School of Physical Sciences, University of Kent. G.M. acknowledges support by the Royal Society under University Research Fellowship Award No. URF\R\180004.

Data availability. The computer codes used to generate the data supporting the findings in this article are openly available [32].

[1] P. Hohenberg and W. Kohn, Inhomogeneous electron gas, Phys. Rev. **136**, B864 (1964).

[2] T. K. Ng, Generalized Hohenberg-Kohn theorem and effective Hamiltonian of a quantum system, Phys. Rev. B **44**, 2407 (1991).

[3] J. Quintanilla, Relationship between the wave function of a magnet and its static structure factor, Phys. Rev. B **106**, 104435 (2022).

[4] B. Murta and J. Fernández-Rossier, One-to-one correspondence between thermal structure factors and coupling constants of general bilinear Hamiltonians, Phys. Rev. E **105**, L062101 (2022).

[5] B. Swingle and I. H. Kim, Reconstructing quantum states from local data, Phys. Rev. Lett. **113**, 260501 (2014).

[6] M. Cramer, M. B. Plenio, S. T. Flammia, R. Somma, D. Gross, S. D. Bartlett, O. Landon-Cardinal, D. Poulin, and Y.-K. Liu, Efficient quantum state tomography, Nat. Commun. **1**, 149 (2010).

[7] E. Chertkov and B. K. Clark, Computational inverse method for constructing spaces of quantum models from wave functions, Phys. Rev. X **8**, 031029 (2018).

[8] M. Greiter, V. Schnells, and R. Thomale, Method to identify parent Hamiltonians for trial states, Phys. Rev. B **98**, 081113(R) (2018).

[9] E. Bairey, I. Arad, and N. H. Lindner, Learning a local Hamiltonian from local measurements, Phys. Rev. Lett. **122**, 020504 (2019).

[10] X.-L. Qi and D. Ranard, Determining a local Hamiltonian from a single eigenstate, Quantum **3**, 159 (2019).

[11] X. Turkeshi, T. Mendes-Santos, G. Giudici, and M. Dalmonte, Entanglement-guided search for parent Hamiltonians, Phys. Rev. Lett. **122**, 150606 (2019).

[12] A. Anshu, S. Arunachalam, T. Kuwahara, and M. Soleimanifar, Sample-efficient learning of interacting quantum systems, Nat. Phys. **17**, 931 (2021).

[13] R. Coldea, D. A. Tennant, E. M. Wheeler, E. Wawrzynska, D. Prabhakaran, M. Telling, K. Habicht, P. Smeibidl, and K. Kiefer, Quantum criticality in an Ising chain: Experimental evidence for emergent E_8 symmetry, Science **327**, 177 (2010).

[14] O. Breunig, M. Garst, A. Klümper, J. Rohrkamp, M. M. Turnbull, and T. Lorenz, Quantum criticality in the spin-1/2 Heisenberg chain system copper pyrazine dinitrate, Sci. Adv. **3**, eaao3773 (2017).

[15] See Supplemental Material at http://link.aps.org/supplemental/10.1103/x9mb-x1gz for further details on our approach to sampling the fitness landscape; the chosen metrics for scattering function and state spaces; sampling random pure states or density matrices near a target state; extending the theorems underpinning Hamiltonian learning and quantum state tomography from magnetic structure factors to Hamiltonians with arbitrary local magnetic fields; and extending these proofs to finite magnetic clusters, which includes Refs. [33–37].

[16] J. Schnack, in *Computational Modelling of Molecular Nanomagnets*, edited by G. Rajaraman (Springer, Cham, 2023), pp. 155–177.

[17] A. Kandala, A. Mezzacapo, K. Temme, M. Takita, M. Brink, J. M. Chow, and J. M. Gambetta, Hardware-efficient variational quantum eigensolver for small molecules and quantum magnets, Nature (London) **549**, 242 (2017).

[18] An analysis of the difficulty of proving this rigorously has been offered in Ref. [4].

[19] F. Becca and S. Sorella, *Quantum Monte Carlo Approaches for Correlated Systems* (Cambridge University Press, Cambridge, UK, 2017).

[20] K. Capelle, A bird's-eye view of density-functional theory, Braz. J. Phys. **36**, 1318 (2006).

[21] P. O. Scherer, *Computational Physics* (Springer, Berlin, 2010).

[22] G. Carleo and M. Troyer, Solving the quantum many-body problem with artificial neural networks, Science **355**, 602 (2017).

[23] J.-G. Liu, L. Mao, P. Zhang, and L. Wang, Solving quantum statistical mechanics with variational autoregressive networks and quantum circuits, Mach. Learn.: Sci. Technol. **2**, 025011 (2021).

[24] H. Ott, Single atom detection in ultracold quantum gases: A review of current progress, Rep. Prog. Phys. **79**, 054401 (2016).

[25] M. F. Parsons, A. Mazurenko, C. S. Chiu, G. Ji, D. Greif, and M. Greiner, Site-resolved measurement of the spin-correlation function in the Fermi-Hubbard model, Science **353**, 1253 (2016).

[26] Y. A. Alaoui, B. Zhu, S. R. Muleady, W. Dubosclard, T. Roscilde, A. M. Rey, B. Laburthe-Tolra, and L. Vernac, Measuring correlations from the collective spin fluctuations of a large ensemble of lattice-trapped dipolar spin-3 atoms, Phys. Rev. Lett. **129**, 023401 (2022).

[27] P. Willke, Y. Bae, K. Yang, J. L. Lado, A. Ferrón, T. Choi, A. Ardavan, J. Fernández-Rossier, A. J. Heinrich, and C. P. Lutz, Hyperfine interaction of individual atoms on a surface, Science **362**, 336 (2018).

[28] R. J. G. Elbertse, D. Coffey, J. Gobeil, and A. F. Otte, Remote detection and recording of atomic-scale spin dynamics, Commun. Phys. **3**, 94 (2020).

[29] S.-h. Phark, Y. Chen, H. T. Bui, Y. Wang, M. Haze, J. Kim, Y. Bae, A. J. Heinrich, and C. Wolf, Double-resonance spectroscopy of coupled electron spins on a surface, ACS Nano **17**, 14144 (2023).

[30] Y. del Castillo and J. Fernández-Rossier, Certifying entanglement of spins on surfaces using ESR-STM, Phys. Rev. B **108**, 115413 (2023).

[31] V. Zauner, D. Draxler, L. Vanderstraeten, J. Haegeman, and F. Verstraete, Symmetry breaking and the geometry of reduced density matrices, New J. Phys. **18**, 113033 (2016).

[32] T. Tula, G. Möller, and J. Quintanilla, Tymoteusz-tula/fitnesslandscape: V1.0.2, Zenodo (2025), https://doi.org/10.5281/zenodo.16844743.

[33] H. R. Irons, J. Quintanilla, T. G. Perring, L. Amico, and G. Aeppli, Control of entanglement transitions in quantum spin clusters, Phys. Rev. B **96**, 224408 (2017).

[34] C. Broholm, Neutron scattering, correlation functions & linear response functions, Lecture notes (2010), https://neutrons2.ornl.gov/conf/nxs2013/lecture/pdf/SS-2013BroholmMagneticNeutronScattering.pdf.

[35] E. Ising, Beitrag zur Theorie des Ferromagnetismus, Ph.D. thesis, University of Hamburg, 1924; Z. Physik **31**, 253 (1925).

[36] S.-J. Gu, G.-S. Tian, and H.-Q. Lin, Ground-state entanglement in the XXZ model, Phys. Rev. A **71**, 052322 (2005).

[37] A. Kitaev, Anyons in an exactly solved model and beyond, Ann. Phys. **321**, 2 (2006).